START-TO-END SIMULATION OF eRHIC ERL*

Yue Hao†, Stephen Brooks, Yichao Jing, François Méot, Vadim Ptitsyn, Dejan Trbojevic,
Nicholaos Tsoupas, BNL, Upton, New York 11973, USA

Abstract

The ERL-ring eRHIC adopts the electron accelerator design of a multi-pass energy recovery linac (ERL), with fixed field alternating gradient (FFAG) recirculating passes. To ensure the beam quality in the accelerating and decelerating stage and the energy recovery efficiency, detailed start-to-end simulation is required to evaluate the various beam dynamics effects, such as synchrotron radiation, wake fields, coherent synchrotron radiation and spin dynamics. In this paper, we present the eRHIC ERL start-to-end simulation strategy with various simulation codes and the current status.

INTRODUCTION

Electron-ion collider is a power tool of deep inelastic scattering for probing the inner structure of the hadrons. To get a much greater insight of the nucleon structure, including the distribution of the momentum, spin and flavor of the quarks and gluons, a high luminosity electron ion collider (EIC) is required.

The nominal design of the EIC in BNL, eRHIC [1], is adding an Energy Recovery Linac to provide electron beam up to 20 GeV. The electron beam with top energy will collide with the ion beam in RHIC. The main advantage of adopting this 'ERL-ring' collision scheme is that higher luminosity can be achieved, since the electron beam collides only once and beam-beam tune shift of the electron beam is not limited by the nonlinear resonances due to beam-beam effect as in a ring-ring scheme collider.

In an ERL, the electron beam gains energy from the RF cavities (usually superconducting) with the accelerating phase. After the electron beam collides with the ion beam, it will be decelerated in the same RF cavity, with the decelerating phase which is ensured by the correct pass length of the electron beam. The energy is then used to accelerate the new electron bunches.

eRHIC ERL adopts a multi-pass ERL design to save cost on the expensive Superconducting RF structure, i.e. the electron beam passes the linac with accelerating phase several times to accumulate energy before collision. To avoid building large number of energy recirculation passes, eRHIC also takes advantage of the concept of FFAG [2], which has enormous momentum acceptance (up to 4x in the design), to reduce the number of recirculation beamlines to two lines. The FFAG based ERL reduces the cost of the transport lines significantly.

* Work supported by Brookhaven Science Associates, LLC under Contract No. DE-AC02-98CH10886 with the U.S. Department of Energy.

† yhao@bnl.gov

Table 1: The Baseline Parameters of ERL-Ring eRHIC

Parameters	Values
Injection energy (GeV)	0.02
Top energy (GeV)	20
Energy gain of linac (GeV)	1.66
Main cavity frequency (MHz)	647
E-loss compensation cavity freq. (MHz)	1294
Rms bunch length (mm)	3
No. of passes	12
No. of FFAG line	2
No. of passes in low energy FFAG	3
No. of passes in high energy FFAG	9
rms norm. emit. (mm-mrad)	23

ERL START-TO-END SIMULATION

It is essential to perform start-to-end simulation of the multi-pass FFAG based ERL to ensure energy recovery process and the beam quality. Two codes are now being used for this purpose, Elegant [3,4] and Zgoubi [5,6]. In Elegant, we use uses 4th order symplectic integrator to track the particles with large momentum deviation with wake field effects. Zgoubi is a stepwise ray-tracing code, its integrator is based on Taylor series methods. Zgoubi also provides the unique feature of spin tracking.

The parameters used in simulations are listed in Table 1.

Studies using Elegant

In Elegant, we model the entire energy recovery process from the injection energy to the top energy with 12 times passing through the linac, then 12 times decelerating through the same linac to the dump energy. In the linac, both the 650MHz fundamental cavities and the second harmonic cavity are included. The voltage of the fundamental cavities is set to achieve the designed energy gain of linac for on crest electrons, while the voltage of the second harmonic cavity is determined by compensating the accumulated energy loss due to synchrotron radiation. Since the energy compensation is evenly distributed into 24 pass through the linac and the energy losses due to synchrotron radiation sharply depend on the beam energies, there will be energy difference (up to 2%) between the accelerating and decelerating bunches in the same recirculating pass.

In the FFAG transport lines, we use 4th order symplectic integrator elements and exact drift element to track the particles since, in FFAG, the particle has large momentum deviation with respect to the reference energy of the beamline.

The connections between FFAG lines and the linac are sets of (12) spreaders and combines. They are designed to match

ISBN 978-3-95450-147-2

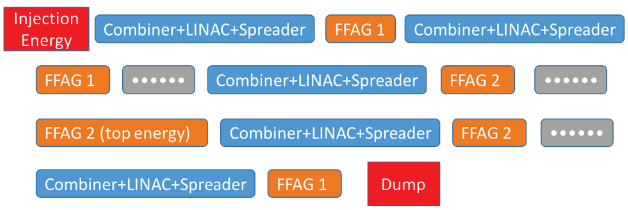

Figure 1: The components and sequence of start-to-end simulation.

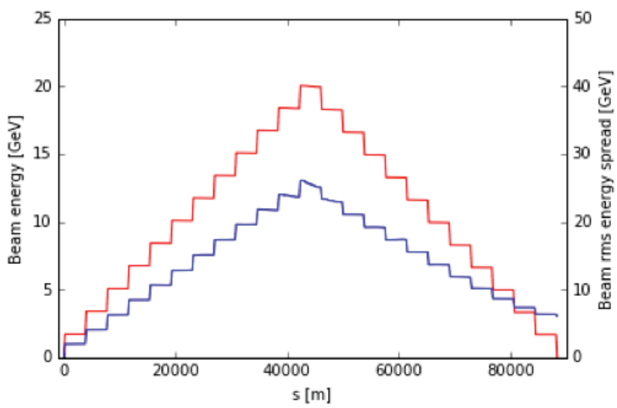

Figure 2: The beam energy(red) and rms energy spread(blue) of the electron beam through the start-to-end transport.

the optics functions, as well as provide correct path length for acceleration/deceleration and the compaction factors. A full design of the spreaders/combiners is not finished. Therefore, in elegant simulation, they are represented by the 6-D linear transfer matrix elements to match the optics function, and the compaction factor, the same element also allows the time of flight change to control the beam phase when the beam passes through the linac next time.

The longitudinal dynamics of a multi-pass ERL is essential to guarantee the energy recovery process. Ideally, the pass length of the all recirculating passes should be $n\lambda$ (lower energy passes) and $(n + 1/2)\ \lambda$(highest energy pass) and the pass length does not depend on the energy of the electron, i.e. the compaction factor and its higher order terms are zero. In eRHIC ERL, we use the spreader and combiner to compensate the pass length and compaction factor ($dl/d\delta$) for the design energy, of each pass. The start-to-end simulation will evaluate the effects of the higher order terms.

Figure 2 shows the energy and rms energy spread of the electron beam in the start-to-end simulation. The energy spread of the electron is contributed from the RF curvature and the synchrotron radiation. The RF induced energy spread, when the beam is accelerated on-crest, can be calculated as

$$\frac{\Delta E}{E} = \frac{1 - \exp\left(-k_{RF}^2 \sigma_z^2\right)}{\sqrt{2}}$$

,which can be compensated in the decelerating stage if the decelerating phase is π apart. The residue energy spread is

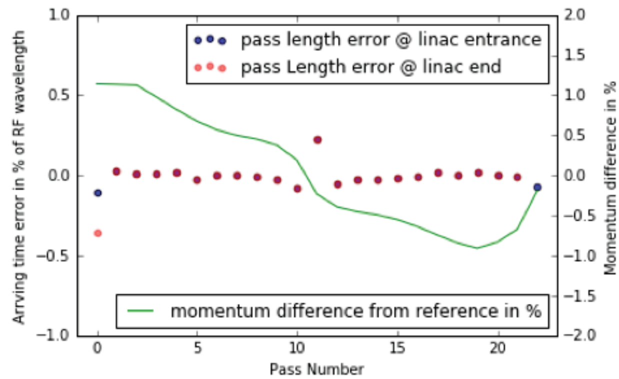

Figure 3: The pass length of error of each pass as function of pass number (blue and orange dots). The blue dots are measured at the linac entrance and the orange dots are measured at the linac exit. The green curve represents the momentum difference in each pass.

Table 2: Longitudinal Dynamics Tolerance

	Tolerance
Pass length (in unit of 647MHz wavelength)	3e-4
Compaction factor (cm)	5

dominated by the synchrotron radiation effect which can not be compensated.

Figure 3 shows the arriving time of each energy pass in fraction of the wavelength of the cavity (the dots) and the energy deviation from the design energies of the electron beam. Not all fractions of the arriving time are zero. The first two dots in the plot reflect the difference of the time of flight between measuring at the entrance and the exit of the linac. The difference is due to the non-ultra relativistic beam at the injection energy. The time of flight of the highest energy (pass 12) and the R_{56} of pass 1, 2, and 3 are adjusted to minimize the energy spread at the dump energy (after pass 24).

If the setting, corresponding to figure 2 and 3, is set as reference, the start-to-end simulation can determine to tolerance of the rms error of the pass length and the compaction factor, which is summarized in table 2. The tolerance is set by limiting the energy spread increase at dump energy to be no more than 20% and the results are averaged over 30 random seeds. We have to control the error sources, including the FFAG magnet misalignment and gradient error to achieve these requirements.

The transverse effects can also be studied in the start-to-end manner. The most challenging effect is the high chromaticity (few hundred units) in non-scaling FFAG arc and chromaticity induced emittance growth [7, 8]. Figure 4 represents an example of emittance growth and orbit deviation with applying 0.1 micron rms magnet displacement error on all FFAG magnets. The emittance growth is due to the chromatic effect when beam deviates from its ideal orbit. We may establish the orbit correction goal, as shown in Table

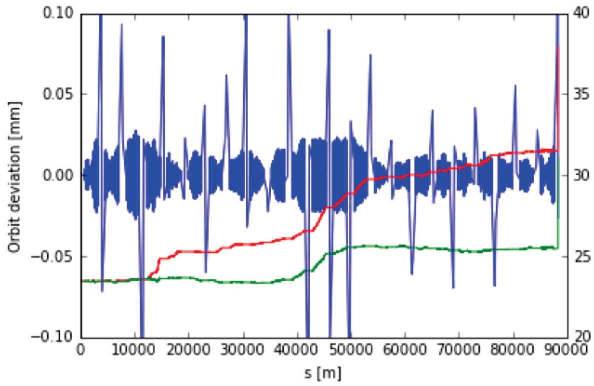

Figure 4: The start-to-end emittance growth due to the magnet misalignment errors (red line), compared with the case without errors (gree line). The orbit deviation is plotted in blue lines.

Table 3: Transverse Emittance Growth Tolerance

	Tolerance
Maximum orbit distortion (μm)	20
Maximum dispersion distortion (mm)	5

3, to avoid more than 20% emittance growth at interaction point from significant luminosity loss.

The tight tolerance due to the large chromatic effect, achieved from the start-to-end simulation encourages an re-consideration of the design of the non-scaling FFAG, to reduce the chromaticity.

Studies using Zgoubi

Start-to-end simulations in Zgoubi include the fundamental RF cavities, the FFAG lattice and spreader/combiner lines that optically match the linac and the multiple-orbit FFAG channels.

A complete high-energy loop in an earlier FFAG design (12 linac passes, 6.6 to 21.2 GeV, 1.3~GeV linac) has been studied [9, 10], some results are discussed here as an illustration. Figure 5 shows details of the optical functions in the linac region (β_x, β_y parabolas in the linac proper), including a merger line (left of the linac) and a spreader line (right); these lines include beam steering respectively from

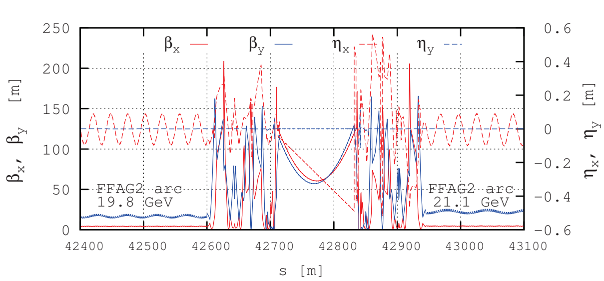

Figure 5: Details of the optical functions in linac region, 19.842 → 21.164 GeV pass.

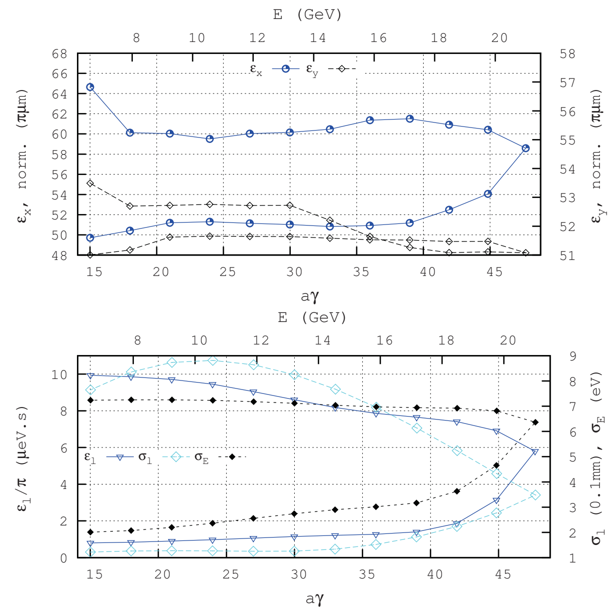

Figure 6: 6-D evolution of a bunch. Top: transverse emittances. Bottom: longitudinal emittance and σ_l, σ_E.

and onto the 19.842 and 21.164 GeV orbits in the FFAG (earlier version); the ±10 cm oscillation of the dispersion in the FFAG is due to cumulated upstream mismatch. Figure 6 shows the evolution of bunch size over a 23-loop accelerated/decelerated cycle, with starting initial rms conditions $\epsilon_x = \epsilon_y = 50\pi\,\mu$m, $\delta E/E = 3 \times 10^{-4}$; transverse growth is essentially due to chromaticity in the presence of residual orbit mismatch in the FFAG. These are some of the ingredients in a 6D+spin, multi-particle, start-to-end simulation detailed in [10], which constitutes the ground work for future eRHIC simulations.

OUTLOOKS

eRHIC ERL start-to-end simulation is an on-going effort to model all elements and multiple physics effects to prove the feasibility of the design. The current results indicate that tight transverse tolerance, that prevents the emittance growth due to large chromaticity, is main challenge in the multi-pass ERL design. The chromaticity reduction study is under way.

In the meantime, we are developing new machine commissioning and correction scheme for the FFAG based multi-pass ERL, including the transverse orbit correction scheme and the pass length/compaction factor correction scheme. These methods will be implemented in the start-to-end simulation.

Currently, we use the ERL injection energy (20MeV) as the starting point of the simulation. After the eRHIC injector is fully modeled, the realistic beam distribution can be used as input for the energy recovery process. At the same time, the real distribution of the exhausted electron beam, at the dump energy, will be use for the design of the ERL beam dump.

ISBN 978-3-95450-147-2

REFERENCES

[1] arXiv:1409.1633

[2] D. Trbojevic, et al, “Non-Scaling Fixed Field Alternating Gradient ERL for eRHIC”, in proceedings of IPAC 2015, Richmond, VA

[3] M. Borland, ’elegant: A Flexible SDDS-Compliant Code for Accelerator Simulation’, Advanced Photon Source LS-287, September 2000.

[4] Y. Wang and M. Borland, "Pelegant: A Parallel Accelerator Simulation Code for Electron Generation and Tracking", Proceedings of the 12th Advanced Accelerator Concepts Workshop, AIP Conf. Proc. 877, 241 (2006).

[5] F. Méot, The ray-tracing code Zgoubi - Status, NIM A 767 (2014) 112125;

[6] F. Méot, Zgoubi users guide, `http://www.osti.gov/scitech/biblio/1062013`

[7] V.N. Litvinenko, Y. Hao and Y.Jing, “Chromatic Effects in Long Periodic Transport Channels”, in the proceedings of IPAC 2015, Richmond, VA

[8] End-to-end polarized bunch transport in eRHIC, F. Méot, FFAG’14 Workshop, BNL, `https://www.bnl.gov/ffag14/`

[9] Tracking studies in eRHIC energy-recovery recirculator, F. Méot, S. Brooks, V. Ptitsyn, D. Trbojevic, N. Tsoupas, BNL/C-AD Note C-A/eRHIC/45 (July 2015)

[10] eRHIC ERL modeling in Zgoubi, F. Méot, S. Brooks, Y. Hao, Y. Jing, V. Ptitsyn, D. Trbojevic, N. Tsoupas, BNL/C-AD Note C-A/eRHIC/49 (Jan. 2016)